Acta Geochim (2021) 40(5):773–786
https://doi.org/10.1007/s11631-021-00465-3

ORIGINAL ARTICLE

Geochemistry, geochronology, and zircon Hf isotopic compositions of felsite porphyry in Xiangshan uranium orefield and its geological implication

Mingming Tian[1] · Ziying Li[1] · Jiangtao Nie[1] · Jun Zhong[1] · Jian Wang[1] · Jianhui Cao[1]

Received: 8 September 2020 / Revised: 24 January 2021 / Accepted: 25 February 2021 / Published online: 12 March 2021

Abstract Recently, a new kind of volcanic rock, felsite porphyry, has been revealed by drilling in Xiangshan area, Jiangxi Province, China. To better understand petrogenesis and magmatic evolution sequence of the Xiangshan volcanic-intrusive complex, we studied systematic petrology, geochemistry, LA-ICP-MS zircon U–Pb dating, and Hf isotope results of the felsite porphyry. Results show that the felsite porphyry has similar geochemical characteristics to the porphyroclastic rhyolite, which is the predominant lithology of Xiangshan uranium orefield. Felsite porphyry and porphyroclastic rhyolite have high SiO_2, Al_2O_3, and K_2O contents, low Na_2O, and MgO contents, and slightly negative Eu anomalies. Moreover, these rocks are relatively depleted in large ion lithophile elements (K, Ba, and Sr) and are enriched in high field strength elements (Th, Zr, and Hf). LA-ICP-MS zircon U–Pb dating of the felsite porphyry yielded a crystallization age of 132.2 ± 0.9 Ma, which is coeval to that of the porphyroclastic rhyolite. These ages signified that Xiangshan volcanic-intrusive complex formed in the Early Cretaceous, during which the entire South China was in the back-arc extension tectonic setting related to the subduction of the Pacific Plate under the Euroasian Plate. *In-situ* zircon Hf isotope data on a felsite porphyry sample show $\varepsilon_{Hf}(t)$ values from − 8.82 to − 5.11, while the Hf isotope two-stage model age ($T_{DM2\text{-}Hf}$) ranges from 1513 to 1747 Ma. Combined with petrological, mineralogical, geochemistry, and geochronology results of the felsite porphyry, it is concluded that the felsite porphyry in Xiangshan might be originated from the partial melting of the Mesoproterozoic ancient metamorphic rocks, with possible input of small amounts of mantle materials.

Keywords Petrogeochemistry · LA-ICP-MS zircon U–Pb age · Hf isotope · Felsite porphyry · Xiangshan uranium orefield

1 Introduction

Xiangshan uranium orefield in Jiangxi Province is the largest volcanic type uranium orefield in China, which attracted great attention and systematic studies focusing on petrology, mineralogy, ore geology, geochemistry, and geochronology (Fang et al. 1982; Liu et al. 1990; Wang et al. 1991; Xia et al. 1992; Chen et al. 1999; Wu, 1999; Wu et al. 2003; Fan et al. 2005, 2009; Zhang and Li 2007; Zhang 2016; Yang et al. 2009, 2010; Li et al. 2014; Wu et al. 2017). Previous studies show that the volcanic activities in Xiangshan occurred from the Late Jurassic to the Early Cretaceous and lasted for ~ 30 Ma from 160 to 130 Ma. In addition, most researchers believe that the volcanic-intrusive complex is mainly derived from the partial melting of felsic crust (Fan et al. 2001a; Jiang et al. 2005; Yang et al. 2011; Guo et al. 2016; Yu et al. 2019). However, whether the rocks have the same source and whether mantle material was added or not remain to be controversial. Some scholars believe that all kinds of volcanic and sub-volcanic rocks in Xiangshan are products of partial melting of the same or similar magma source (Fang et al. 1982; Fan et al. 2001a; Jiang et al. 2005; Yang et al.

Supplementary Information The online version contains supplementary material available at https://doi.org/10.1007/s11631-021-00465-3.

✉ Mingming Tian
tian_ming_ming@126.com

[1] Beijing Research Institute of Uranium Geology, Beijing 100029, China

2011). Others believe that Xiangshan volcanic-intrusive complex was derived from a different magma source, with the input of mantle materials (Fan et al. 2001b; Guo et al. 2016). Different lithologies, including the acidic porphyroclastic rhyolite, rhyodacite, granitic porphyry, dacite porphyry, rhyolitic porphyry (Fan et al. 2009; Yang et al. 2009, 2010; Zhou and Wang 2012; Wu et al. 2017; Zhang 2016; Zhang et al. 2018; He et al. 2009; Yang et al. 2009, 2010; Yang 2013; Ruan 2018; Si et al. 2018) and mafic dykes like lamprophyre (Wang 2015; Wang et al. 2019), were recognized and analyzed. Recently, a new type of concealed rocks, the felsite porphyry, was found from the boreholes in Heyuanbei and Lejia of mid-western Xiangshan area. Guo et al. (2014) conducted preliminary isotopic dating on the felsite porphyry intercepted by scientific deep drilling in the Xiangshan uranium orefield. However, the petrogenesis remains poorly constrained, which hindered our understanding of the Xiangshan volcanic-intrusive complex. Therefore, in this manuscript, we present a systematic study of felsite porphyry on petrology, mineralogy, geochemistry, zircon U–Pb geochronology, and zircon Hf isotope geochemistry, to better understand the petrogenesis of the Xiangshan volcanic-intrusive complex.

2 Geological settings

Xiangshan uranium orefield is located in the Jiangxi Province. Geotectonically, it lies within the Gan-Hang tectonic belt, which is close to the tectonic suture zone between the Yangtze plate and the Cathaysia plate (Fig. 1). Xiangshan volcanic-intrusive complex, appearing as ellipses in-plane, occupies an area of about 309 km^2, with length (east–west) of about 26.5 km, and width (north–south) of about 15 km. It is regarded as a large volcanic collapsed basin (Xia et al. 1992; Zhang 2011), which can be divided into three layers: the basement mainly composed of Early-Middle Proterozoic and Sinian metamorphic rocks, with local occurrences of the Lower Carboniferous and Upper Triassic series; The volcanic rocks are the major lithologies formed in Cretaceous in Xiangshan, and mainly composed of the rhyolitic crystal tuff, rhyolitic ignimbrite and rhyodacite of the Daguding Formation (K_1d), and porphyroclastic rhyolite, granitic porphyry, rhyolitic dacite porphyry, quartz-monzonite porphyry and amprophyre of the Ehuling Formation (K_1e). Of all the volcanic rocks, the porphyroclastic rhyolite is the predominant lithology and the host rocks of the uranium deposits in the Xiangshan basin. The Cretaceous red bed cover mainly includes sandstone and sandy conglomerate and the latest rocks recognized in the Xiangshan basin.

3 Samples and analytical methods

The felsite porphyry samples analyzed in this study were collected from the scientific deep drilling borehole CUSD3 in the Heyuanbei area and borehole CUSD4 in the Lejia area, in the midwestern Xiangshan area (Fig. 1). The samples are relatively fresh without alteration. The color of felsite porphyry is caesious. Felsite-porphyritic texture and massive structure (Fig. 2a), some late carbonate veinlets and microfissures can be found (Fig. 2b, f). The results of rock-mineral identification show that phenocrysts account for 25%–30%, which is dominated by quartz and sanidine, plagioclase followed. The quartz is mainly in the form of allotrimorphic granular, with a particle size of 1–3 mm and a content of about 17%, in addition, embayment phenomenon can be seen occasionally (Fig. 2c, d), but no obvious catalastic texture. Potash feldspar is in the shape of allotrimorphic-subeuhedral tabular, with a particle size of 1.5–3.5 mm and a content of about 13%, albitization, and chloritization alteration can be seen locally. While the plagioclase shows a higher degree of euhedral, mainly in the form of euhedral-subeuhedral tabular, 2–4 mm, with a content of about 12%, sericitization occurs on some plagioclases (Fig. 2e). The matrix accounts for 65%–70%, and mainly composed of feldspar-quartz minerals and a small amount of biotite, with uneven crystal granularity, the matrix also shows felsite texture, and the average particle size is less than 0.2 mm, some are less than 0.01 mm.

3.1 Major and trace elements analysis

The major and trace element compositions of the samples were analyzed in the Analytic Laboratory of Beijing Research Institute of Uranium Geology (ALBRIUG). Before testing, the samples were firstly ground into 200 mesh. Major elements test was performed by the PW2404 X-ray fluorescence spectrometer. The specific operation is Using the XRF fluorescence spectrometer to analyze after the powder samples were made into a deplanate glass sheet, the analysis accuracy was better than 5%. Trace elements and REE were analyzed by plasma mass spectrometer (ICP-MS), and the sample processing method was as followed: Firstly, weighted 200 mg powder sample, mixed with a 900 mg $LiBO_2$ flux uniformly, then melting in a furnace at 1000 °C. Secondly, dissolving and diluting the melt with 100 mL 4% nitric acid after the melt was cooled, and then analyzing with ICP-MS, the analysis accuracy is 5%–10%.

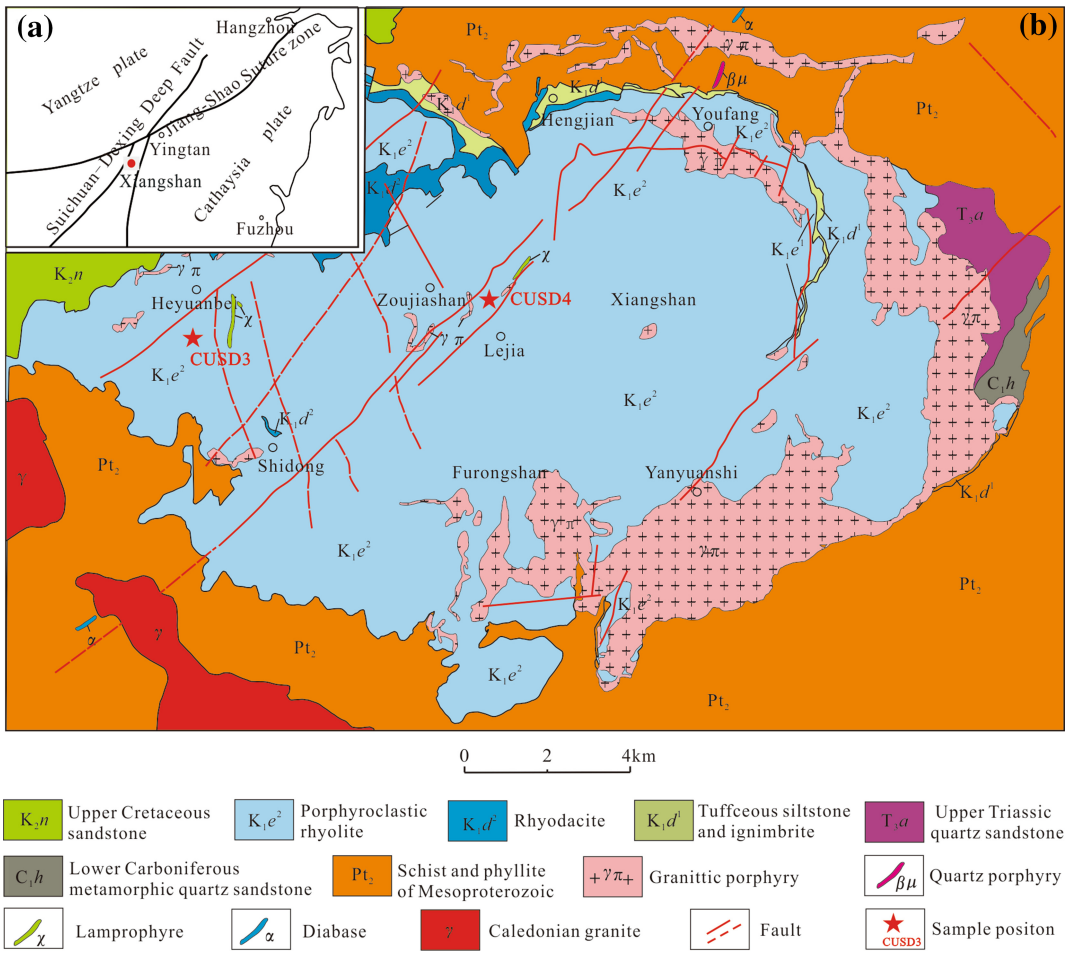

Fig. 1 Geotectonic location **a** and geological sketch map **b** of Xiangshan uranium orefield (Modified after Wang et al. 2019)

3.2 LA-ICP-MS zircon U–Pb analysis

Zircons used for U–Pb dating were extracted from felsite porphyry powder samples using electromagnetic separation and heavy liquid suspension at the testing and analysis center of Beijing Research Institute of Uranium Geology. Then preferable crystal and representative zircons were selected under a microscope. The process of zircon targets, transmitted light, reflected light and cathode luminescence (CL) images were completed by Beijing Zirconium Technology co., Ltd. Based on the above process, zircon images were systematically studied, and the structure, texture, microfissures, and inclusions were identified clearly. Preferable crystal, clear crystal edge, and transparent magmatic zircons were selected for testing. LA-ICP-MS zircon U–Pb dating experiment was undertaken at State Key Laboratory of Continental Dynamics, Northwest University, Xi'an, China. The instrument model is Agilent7500 ICP-MS, which is equipped with ComPex102 ArF excimer laser (working substance is ArF and the wavelength is 193 nm) and GeoLas200M optical system. During the experiment, Helium was used as the carrier gas of the denudation material. U concentration and U/Pb fractionation value of the unknown samples were corrected by alternating measured values of standard reference material for artificial silicate glass NISTSRM610 from the National Institute of Standards and Technology (NIST) and the standard zircon 91500 from Harvard University. Raw data were processed using the GLITTER program, and the uncertainties of individual analyses are reported with 1σ error. Weighted mean ages were calculated at 1σ confidence level. The correction of normal lead by Anderson's method (Anderson 2002), and the age calculation was completed by national standard program Isoplot ver3.0 (Ludwing 2003).

3.3 Zircon Hf isotope analysis

Zircon Lu–Hf isotope *in-situ* analysis was also conducted at the State Key Laboratory of Continental Dynamics, Northwest University, Xi'an, China. The Nu Plasma HR multi-reception inductively coupled Plasma mass

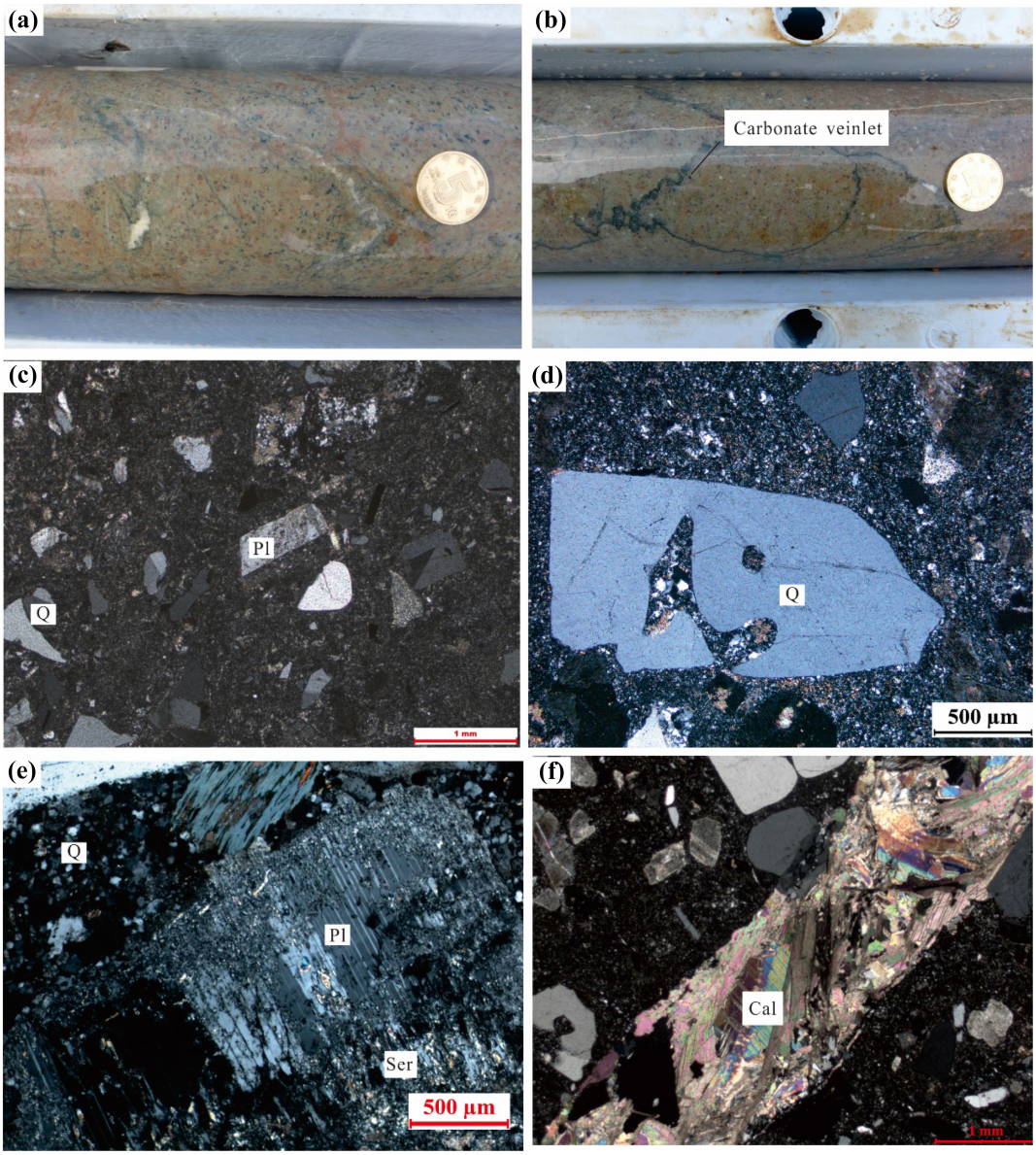

Fig. 2 Photographs showing the felsite porphyry core samples and major rock mineral composition. **a** Felsite porphyry core samples; **b** Carbonate veinlets; **c** Micrographs of felsite porphyry (cross polarized light); **d** Embayment of quartz in felsite porphyry (cross polarized light); **e** Sericitization of plagioclase (cross polarized light); **f** Micrographs of late carbonate veinlet (cross polarized light)

spectrometer (MC-ICP-MS) was used to complete zircon Lu–Hf isotope *in-situ* analysis which is near the U–Pb dating site. For Lu–Hf isotope measurement, $^{176}Lu/^{175}Lu = 0.02669$ and $^{176}Yb/^{172}Yb = 0.5886$ were used for isobaric interference to correct and calculate the ratio of $^{176}Lu/^{177}Hf$ and $^{176}Hf/^{177}Hf$ of the samples. During the testing process, the standard zircon samples 91500 and GJ1 were also tested and analyzed for instrumental quality control and sample calibration. In the calculation of $\varepsilon_{Hf}(t)$, the recommended decay constant value of ^{176}Lu is 1.867×10^{-11} year^{-1}, the $^{176}Lu/^{177}Hf$ and $^{176}Hf/^{177}Hf$ values of the primitive mantle are 0.0332 and 0.282772 respectively (Blichert et al. 1997), and the depleted mantle model age of zircons Hf isotope was calculated using current $(^{176}Hf/^{177}Hf)_{DM} = 0.028325$ and $(^{176}Lu/^{177}Hf)_{DM} = 0.0384$.

4 Results

4.1 Major element analysis results

The major element results of felsite porphyry are listed in supplementary material Table 1. It is shown that the rock is characterized by the enrichment of SiO_2 (72.53 wt% to 76.80 wt%), Al_2O_3 (11.81 wt% to 13.37 wt%), and K_2O,

while depleted in Na_2O and MgO. The total alkali ($Na_2O + K_2O$) ranges from 5.59 wt% to 8.00 wt%, and the Na_2O/K_2O ratio is 0.43–0.86. Compared to the predominant porphyroclastic rhyolite and rhyodacite, the main lithology of Xiangshan area (listed in supplementary material Table 1), felsitic porphyry shows similar major element characteristics with porphyrocalstic rhyolite, while few differences compared with rhyodacite, SiO_2 in felsite porphyry is higher, while Al_2O_3, Fe_2O_3, and FeO are relatively lower. Previous studies have been conducted on the characteristics of the major elements of intermediate-acid dykes in the Xiangshan area, including dacite porphyry, granitic porphyry (Ruan 2018; Wang et al. 2019) (listed in supplementary material Table 1), compared with felsite porphyry, the results show that felsite porphyry presented by significantly higher SiO_2, while lower Al_2O_3, Fe_2O_3, and FeO. In the TAS classification diagram of volcanic rocks (Fig. 3), felsite porphyry, porphyroclastic rhyolite, and rhyolitic porphyry samples all fell in the rhyolite region. In the SiO_2-AR classification diagram, all of the samples fell into the cal-alkaline region (Fig. 4).

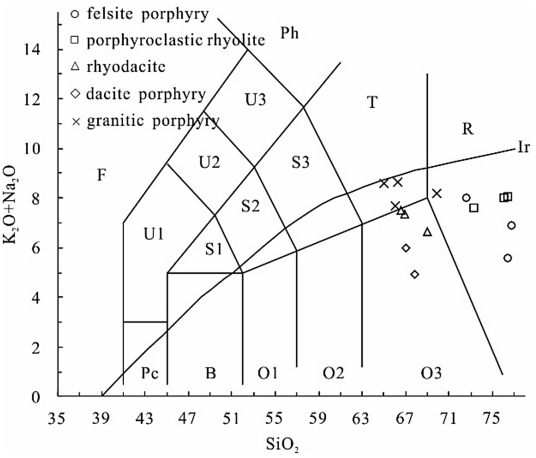

Fig. 3 TAS classification diagram of felsite porphyry (after Le Maitre 1989). Pc-Oceanite; B-Basalt; O1-Basaltic andesite; O2-Andesite; O3-Dacite; R-Rhyolite; S1-Trachybasalt; S2-Basaltic trachyandesite; S3-Trachyandesite; T-Trachite, trachydacite; F-Feldspathoidite; U1-Tephrite, basanite; U2-Phonotephrite; U3-Tephriphonolite; Ph-Phonolite; Ir-Irvine boundary, upper is alkaline and below is subalkaline

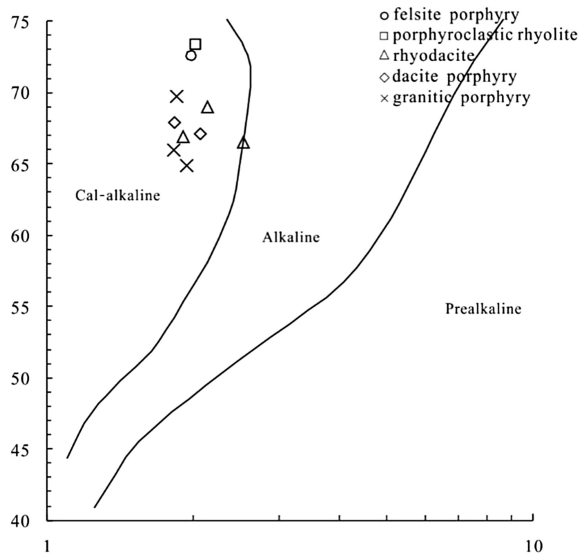

Fig. 4 SiO_2-AR classification diagram (Wright 1969). AR = $[Al_2O_3 + CaO + (Na_2O + K_2O)]/[Al_2O_3 + CaO-(Na_2O + K_2O)]$ (wt%)

4.2 Trace element and REE analysis results

The trace element results are presented in supplementary material Table 2 and Table 3. Compared to porphyroclastic rhyolite, rhyodacite, and intermediate-acid dykes (dacite porphyry, granitic porphyry, and rhyolitic porphyry) in the Xiangshan area (also listed in supplementary material Table 2 and Table 3), felsite porphyry also shows similar trace element composition. On primitive mantle normalized trace element spider diagram (Fig. 5a), felsite porphyry shows almost the same pattern with porphyroclastic porphyry and rhyolitic porphyry, and only a slight difference with rhyodacite, dacite porphyry, and granitic porphyry could be observed. In addition, the felsite porphyry is characterized by the depletion of large ion lithophile elements (LILE, such as K, Ba, Sr) and high field-strength elements (HFSE including Nb, Ti, P), and enrichment of Rb, Th, and Nd. The depletion of Sr and Ba indicated that the rock might undergo strong fractional crystallization of plagioclase, while the losses of P and Ti might be related to the fractional crystallization of apatite and rutile.

The total rare earth element ($\sum$REE) of felsite porphyry concentrations range from 121.39 to 253.67 ppm, with enriched in LREE (LREE/HREE ratio ranges from 8.79 to 11.68) and significant negative Eu anomalies (Fig. 5b, δEu ranges from 0.06 to 0.42). On chondrite normalized REE patterns (Fig. 5b), the felsite porphyry shows a similar distribution pattern to the volcanic-subvolcanic felsic rocks in the Xiangshan area, especially with the porphyroclastic rhyolite. The similar trace element compositions suggest that the felsite porphyry probably share a similar magmatic source and evolution history with the other felsic volcanic rocks in the Xiangshan area, both of which are products of the same magmatic activity at different stages.

4.3 LA-ICP-MS Zircon U–Pb dating analysis

The zircon U–Pb dating sample (SD3-25) was collected from the CUSD3 borehole in Heyuanbei, Xiangshan. Cathode luminescence (CL) images of zircons (Fig. 6)

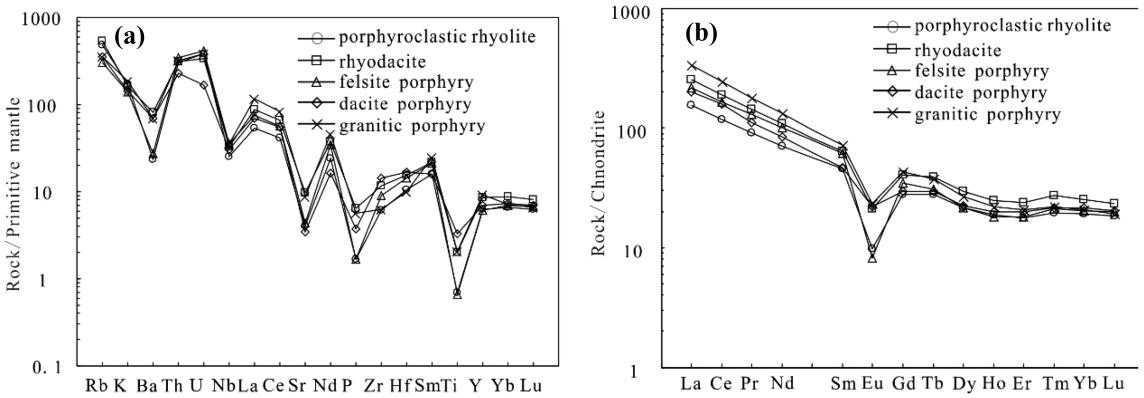

Fig. 5 Primitive mantle normalized trace element spider diagram (**a**) and chondrite normalized REE patterns (**b**) of felsite porphyry (standardized data quote from Sun and McDonough 1989)

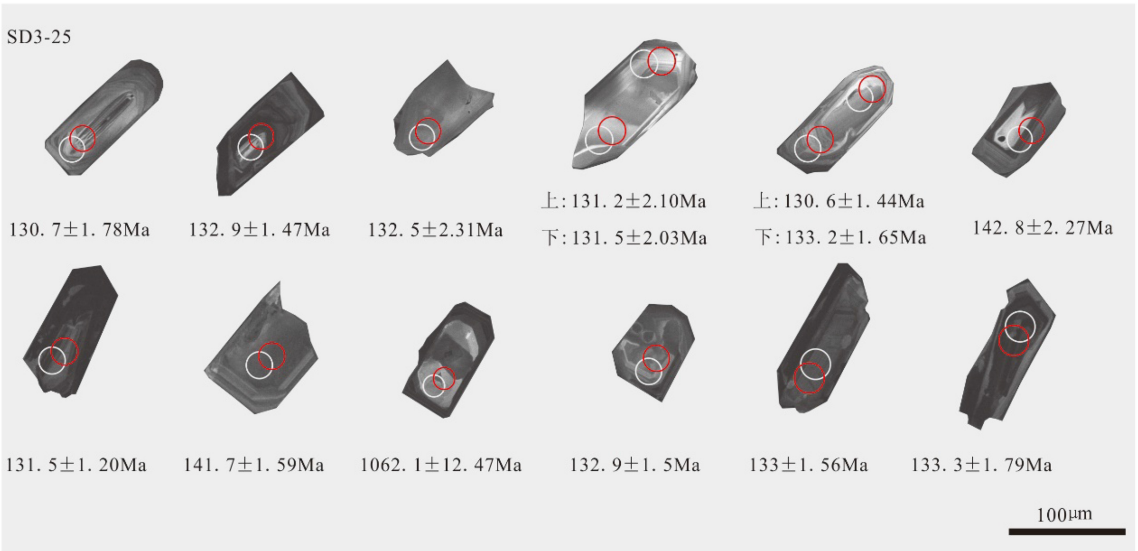

Fig. 6 Zircon CL (cathodoluminescence) images of felsite porphyry. *Note* The white circle and red circle respectively represent the U–Pb dating location and Lu–Hf isotope dating location

show that the zircons are mainly long-columnar and prismatic in shape, with colorless-transparent and yellowish-yellow color. Oscillatory growth zoning could be recognized in most zircon grains, suggesting that the zircons for U–Pb dating are magmatic in origin.

In this study, 14 analyses were performed on 12 zircons from felsite porphyry sample SD3-25 and the results are shown in Table 1 and Fig. 8. The U-Th-Pb analyses yield a range of U and Th concentrations of 43.03–1853.07 ppm and 21.73–664.98 ppm, with an average of 554.89 and 230.06 ppm, respectively. The Th/U ratios range from 0.31 to 1.64 (with an average of 0.58), which is similar to the typical magmatic zircons (Song et al. 2002; Fernando et al. 2003; Samuel and Mark 2003). The U–Pb analyses yield concordant or nearly concordant results within analytical error, with the $^{207}Pb/^{206}Pb$ apparent ages ranging from 130.6 to 142.8 Ma (Table 1). Most zircons have typical oscillatory zones, yielding a concordant $^{206}Pb/^{238}U$ age of 132.2 ± 0.9 Ma (MSWD = 0.38) (Fig. 7). One relatively older age of 1062.1 ± 12.5 Ma in the core of the zircon was recognized (spot 11, Table 1, Fig. 6).

To sum up, the age of felsite porphyry can be constrained to 132.2 ± 0.9 Ma, suggesting that the felsite porphyry is a product of magmatic activity during the Early Cretaceous.

4.4 Zircon Lu–Hf isotopic compositions

Zircon Lu–Hf isotope analysis was performed on the same U–Pb dating zircons and the results are listed in Table 2. Generally, the zircons show very low radiogenic Hf accumulation, and the $^{176}Lu/^{177}Hf$.

ratio can represent the Hf isotope composition during crystallization of the zircons if the $^{176}Lu/^{177}Hf$ ratio is less

Table 1 LA-ICP-MS zircons U–Pb data of felsite porphyry

Sample and spot NO	Concentrations (ppm)		Th/U	Isotopic ratios						Age (Ma)					
	Th	U		$^{207}Pb/^{206}Pb$	1σ	$^{207}Pb/^{235}U$	1σ	$^{206}Pb/^{238}U$	1σ	$^{207}Pb/^{206}Pb$	1σ	$^{207}Pb/^{235}U$	1σ	$^{206}Pb/^{238}U$	1σ
91500-1	22.92	66.12	0.35	0.07431	0.00211	1.83543	0.04127	0.1791	0.00226	1050	56.23	1058.2	14.78	1062	12.34
GJ-1-1	12.96	205.76	0.06	0.06037	0.00159	0.80417	0.01593	0.09659	0.00114	616.8	55.93	599.2	8.96	594.4	6.68
610-1	453.32	459.85	0.99	0.89757	0.01844	27.6693	0.31374	0.22354	0.00248	5085.1	28.74	3407.4	11.11	1300.5	13.06
SD3-25-1	119.08	298.88	0.40	0.05047	0.00221	0.14251	0.00565	0.02047	0.00028	216.8	98.49	135.3	5.02	130.7	1.78
SD3-25-2	512.93	1669.21	0.31	0.04874	0.00117	0.13999	0.00231	0.02083	0.00023	135.2	55.28	133	2.06	132.9	1.47
SD3-25-3	76.9	119.63	0.64	0.04972	0.0036	0.14241	0.00986	0.02077	0.00037	182	160.64	135.2	8.77	132.5	2.31
SD3-25-4	664.98	1419.9	0.47	0.05041	0.00117	0.14223	0.00219	0.02046	0.00023	213.9	52.81	135	1.95	130.6	1.44
SD3-25-5	228.95	390.83	0.59	0.04773	0.00174	0.13739	0.00436	0.02087	0.00026	84.9	85.34	130.7	3.89	133.2	1.65
SD3-25-6	154.19	171.08	0.90	0.04823	0.00288	0.13704	0.0077	0.0206	0.00032	110.5	135.11	130.4	6.88	131.5	2.03
91500-2	25.25	71.54	0.35	0.07478	0.00206	1.84942	0.03941	0.17933	0.00223	1062.7	54.39	1063.2	14.04	1063.3	12.19
GJ-1-2	12.03	190.84	0.06	0.05953	0.00158	0.80355	0.01609	0.09788	0.00115	586.6	56.66	598.8	9.06	602	6.76
610-2	443.49	449.9	0.99	0.91285	0.01886	27.42903	0.31337	0.21788	0.00242	5108.9	28.87	3398.9	11.19	1270.7	12.83
SD3-25-7	77.59	100.14	0.77	0.04667	0.00339	0.1323	0.00923	0.02055	0.00033	32.4	165.61	126.2	8.27	131.2	2.1
SD3-25-8	77.27	47.03	1.64	0.04844	0.0036	0.14965	0.0107	0.0224	0.00036	120.6	166.43	141.6	9.45	142.8	2.27
SD3-25-9	137.31	277.46	0.49	0.04754	0.00264	0.13516	0.007	0.02061	0.00032	75.8	127.55	128.7	6.26	131.5	2
SD3-25-10	325.07	950.41	0.34	0.04946	0.00125	0.15161	0.00276	0.02223	0.00025	169.7	57.9	143.3	2.43	141.7	1.59
SD3-25-11	21.73	66.19	0.33	0.07483	0.00215	1.84811	0.04205	0.1791	0.00228	1063.8	56.68	1062.8	14.99	1062.1	12.47
SD3-25-12	640.2	1853.07	0.35	0.05402	0.00137	0.1552	0.00285	0.02083	0.00024	371.9	56.1	146.5	2.51	132.9	1.5
SD3-25-13	95.34	234.05	0.41	0.04864	0.00147	0.13986	0.0034	0.02085	0.00025	130.6	69.37	132.9	3.03	133	1.56
SD3-25-14	89.26	170.55	0.52	0.05049	0.00222	0.14542	0.00578	0.02089	0.00028	217.4	98.78	137.9	5.13	133.3	1.79
91500-3	21.18	63.54	0.33	0.07476	0.00215	1.84678	0.04223	0.17912	0.00227	1062.2	56.89	1062.3	15.06	1062.1	12.42
GJ-1-3	12.97	204.3	0.06	0.05954	0.00158	0.7924	0.01585	0.09651	0.00113	586.8	56.73	592.5	8.98	593.9	6.67
610-3	454.83	461.4	0.99	0.91314	0.01895	27.54837	0.31634	0.21876	0.00243	5109.3	29	3403.2	11.25	1275.3	12.86

91500, GJ-1, and 610 represent the standard samples

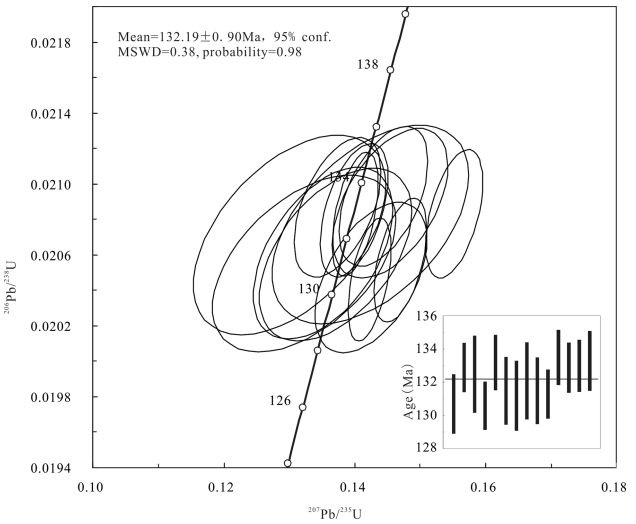

Fig. 7 LA-ICP-MS zircon U–Pb age Concordia diagram and average-weighted age of felsite porphyry

than 0.002 (Hou et al. 2007; Wu et al. 2007). As shown in Table 2, the $^{176}Lu/^{177}Hf$ ratio of felsite porphyry ranges from 0.000620 to 0.001789, $^{176}Hf/^{177}Hf$ ratio ranges from 0.282444 to 0.282548, and the calculated ε_{Hf} (t) value ranges from − 8.82 to − 5.11 (with only one exception of 14.46), and mostly concentrated between − 8 and − 6.5 (Table 2 and Fig. 8a). The single-stage model age of Hf isotope (T_{DM}) ranges from 999 to 1148 Ma, and the two-stage model age (T_{DM2}) ranges from 1513 to 1747 Ma, mostly concentrated between 1500 to 1800 Ma (Fig. 8b).

Meanwhile, the Hf isotope compositions of the porphyroclastic rhyolite of the Ehuling Formation from the Heyuanbei area were also analyzed and the results are listed in Table 2. The calculated ε_{Hf} (t) value varies from − 9.46 to − 4.45, and the two-stage model age (T_{DM2}) varies from 1470 to 1787 Ma, which is extremely close to that of the felsite porphyroclastic rhyolite, indicating the possible same-origin between the felsite porphyry and porphyroclastic rhyolite.

5 Discussion

5.1 The age of felsite porphyry

A series of studies on the formation age of volcanic-intrusive complex of Xiangshan uranium orefield have been carried out in the early stage by K–Ar method and whole-rock Rb–Sr method. The results vary in a large range from 160 to 130 Ma due to the low accuracy of the dating methods (Yu 2001; Wu et al. 2003). Recently, with the development of high-precision isotope dating methods, the formation age of the volcanic-intrusive complex has been constrained to 136–130 Ma (Zhang and Li 2007; He et al. 2009; Yang et al. 2009, 2011; Yang 2013; Chen et al. 2013; Wu et al. 2017). Yang et al. (2010) conducted SHRIMP and LA-ICP-MS zircon U–Pb dating on rhyodacite, and the result is 135.1 ± 1.7 Ma. Meanwhile, the author carried out the LA-ICP-MS zircon U–Pb dating of porphyroclastic rhyolite in Heyuanbei, Xiangshan area, the age ranges from 131.6 Ma to 132.9 Ma (unpublished), these age data indicate that the volcanic-intrusive complex is a product of the same magmatic activity of different stages in the Early Cretaceous, and the rhyodacite is earlier than porphyroclastic rhyolite.

In recent years, a series of relevant studies were performed by some researchers in terms of the formation time of intermediate-acid dykes in Xiangshan uranium orefield. The age of rhyolitic dacite porphyry has been dated to 136.6 ± 2.7 Ma by He et al. (2009) using the SHRIMP U–Pb method, which is relatively consistent with LA-ICP-MS zircon U–Pb dating age of rhyolitic dacite porphyry (134.8 ± 1.1 Ma) by Yang et al. (2010). Ruan (2018) conducted the LA-ICP-MS zircon U–Pb dating on granitic porphyry. The results range from 134 to 136 Ma, which is approximately close to rhyolitic dacite porphyry. Fan et al. (2005) reported the lamprophyre dyke age of 125.1 ± 3.1 Ma by LA-ICP-MS zircon U–Pb dating. Wang et al. (2019) constrained the formation age of late dacite porphyry at Zoujiashan deposit to be 122.4 Ma by LA-ICP-MS zircon U–Pb dating. These ages indicate that multiple contemporaneous dyke magmatic activities occurred after the large-scale magma intrusive activity in the Xiangshan uranium orefield in the Early Cretaceous.

In this study, the LA-ICP-MS zircon U–Pb age of felsite porphyry is 132.2 Ma, which is relatively consistent with that (132 Ma) of the felsite porphyry obtained by Guo et al. (2014) from scientific deep drilling of Xiangshan uranium orefield. It is confirmed that felsite porphyry was formed in the Early Cretaceous, and is much closer to the formation age of porphyroclastic rhyolite, which may be the products of the same-stage magmatic activity.

In conclusion, the large-scale Early Cretaceous volcanic-intrusive activity in the Xiangshan area may be formed in at least three stages within a relatively short period. The magmatic emplacement was initiated by the rhyodacite, rhyolitic dacite porphyry, and granitic porphyry at ∼ 136 Ma, which was followed by the formation of the porphyroclastic rhyolite and felsite porphyry at ∼ 131 Ma. The small-scale magmatic activity of basic and intermediate-acid dykes (such as lamprophyre dyke, dacite porphyry, etc.) formed during 122 ∼ 126 Ma. Marks the termination of the magmatic systems in Xiangshan area.

Table 2 Lu–Hf isotopic data of felsite porphyry and porphyroclastic rhyolite

Sample and spot NO	Age (Ma)	$^{176}Hf/^{177}Hf$	2σ	$^{176}Yb/^{177}Hf$	2σ	$^{176}Lu/^{177}Hf$	2σ	$\varepsilon_{Hf}(0)$	$\varepsilon_{Hf}(t)$	T_{DM}	T_{DM2}	$f_{Lu/Hf}$
Felsite porphyry												
91500-1	1064	0.282340	0.000008	0.007583	0.000004	0.000293	0.000000	− 15.28	8.11	1263	1388	− 0.99
GJ-1-1	603	0.281983	0.000007	0.006188	0.000004	0.000247	0.000000	− 27.9	− 14.72	1748	2470	− 0.99
SD3-25-1	130.7	0.282490	0.000013	0.028087	0.000036	0.001100	0.000001	− 9.99	− 7.21	1081	1646	− 0.97
SD3-25-2	132.9	0.282535	0.000015	0.043135	0.000571	0.001633	0.000020	− 8.39	− 5.61	1032	1546	− 0.95
SD3-25-3	132.5	0.282484	0.000014	0.021938	0.000674	0.000787	0.000015	− 10.17	− 7.35	1079	1654	− 0.98
SD3-25-4	130.6	0.282495	0.000013	0.016680	0.000063	0.000620	0.000002	− 9.8	− 7	1060	1631	− 0.98
SD3-25-5	133.2	0.282548	0.000015	0.028512	0.000221	0.001112	0.000009	− 7.93	− 5.11	999	1513	− 0.97
SD3-25-6	131.5	0.282468	0.000023	0.020850	0.000183	0.000808	0.000007	− 10.76	− 7.94	1103	1692	− 0.98
SD3-25-7	131.2	0.282486	0.000022	0.023078	0.000185	0.000900	0.000007	− 10.12	− 7.31	1081	1653	− 0.97
91500-2	1064	0.282331	0.000008	0.007426	0.000006	0.000287	0.000000	− 15.6	7.79	1275	1408	− 0.99
GJ-1-2	603	0.281962	0.000008	0.006198	0.000004	0.000248	0.000000	− 28.64	− 15.46	1776	2515	− 0.99
SD3-25-8	142.8	0.282477	0.000015	0.016197	0.000163	0.000627	0.000006	− 10.43	− 7.34	1085	1664	− 0.98
SD3-25-9	131.5	0.282444	0.000017	0.031796	0.000123	0.001218	0.000004	− 11.59	− 8.82	1148	1747	− 0.96
SD3-25-10	141.7	0.282495	0.000015	0.020057	0.000306	0.000783	0.000011	− 9.81	− 6.79	1065	1626	− 0.98
SD3-25-11	1062.1	0.282536	0.000015	0.026713	0.000341	0.001019	0.000012	− 8.36	14.46	1014	985	− 0.97
SD3-25-12	132.9	0.282536	0.000012	0.047467	0.000214	0.001789	0.000006	− 8.35	− 5.57	1034	1543	− 0.95
SD3-25-13	133	0.282452	0.000025	0.040255	0.000161	0.001458	0.000006	− 11.32	− 8.54	1145	1731	− 0.96
SD3-25-14	133.3	0.282468	0.000012	0.018659	0.000108	0.000730	0.000004	− 10.75	− 7.9	1101	1691	− 0.98
91500-3	1064	0.282330	0.000007	0.007447	0.000006	0.000288	0.000000	− 15.63	7.76	1276	1409	− 0.99
GJ-1-3	603	0.282060	0.000007	0.006484	0.000003	0.000260	0.000000	− 25.18	− 11.99	1644	2300	− 0.99
Porphyroclastic rhyolite												
91500-4	1064	0.282330	0.000007	0.007447	0.0000006	0.000288	0.000000	− 15.63	7.76	1276	1409	− 0.99
GJ-1-4	603	0.282060	0.000007	0.006484	0.000003	0.000260	0.000000	− 25.18	− 11.99	1644	2300	− 0.99
SD3-62-1	132.6	0.282433	0.000023	0.029988	0.000225	0.001170	0.000008	− 11.98	− 9.18	1161	1769	− 0.96
SD3-62-2	131.7	0.282536	0.000016	0.021733	0.000167	0.000834	0.000006	− 8.35	− 5.52	1008	1539	− 0.97
SD3-62-3	133.7	0.282467	0.000015	0.017610	0.000073	0.000705	0.000003	− 10.78	− 7.92	1100	1690	− 0.98
SD3-62-4	130.9	0.282500	0.000012	0.013598	0.000135	0.000540	0.000006	− 9.61	− 6.78	1049	1616	− 0.98
SD3-62-5	132.4	0.282467	0.000015	0.024355	0.000164	0.000982	0.000002	− 10.80	− 7.99	1108	1692	− 0.97
SD3-62-6	130.6	0.282468	0.000013	0.019147	0.000063	0.000758	0.000006	− 10.76	− 7.95	1100	1690	− 0.98

Table 2 continued

Sample and spot NO	Age (Ma)	$^{176}Hf/^{177}Hf$	2σ	$^{176}Yb/^{177}Hf$	2σ	$^{176}Lu/^{177}Hf$	2σ	$\varepsilon_{Hf}(0)$	$\varepsilon_{Hf}(t)$	T_{DM}	T_{DM2}	$f_{Lu/Hf}$
SD3-62-7	133.4	0.282499	0.000016	0.021721	0.000117	0.000879	0.000005	− 9.66	− 6.80	1060	1619	− 0.97
91500-5	1064	0.282256	0.0000070	0.007350	0.000005	0.000284	0.000000	− 18.25	5.13	1377	1574	− 0.99
GJ-1-5	603	0.282061	0.000008	0.006669	0.000003	0.000267	0.000000	− 25.14	11.96	1643	2298	− 0.99
SD3-62-8	133	0.282509	0.000015	0.030149	0.000085	0.001152	0.000003	− 9.30	− 6.49	1054	1599	− 0.97
SD3-62-9	132.5	0.282538	0.000015	0.026411	0.000088	0.001019	0.000007	− 8.26	− 5.44	1009	1533	− 0.97
SD3-62-10	133.1	0.282451	0.000011	0.016663	0.000201	0.000652	0.000001	− 11.35	− 8.50	1121	1727	− 0.98
SD3-62-11	132.8	0.282424	0.000016	0.012534	0.000019	0.000498	0.000003	− 12.32	− 9.46	1154	1787	− 0.99
SD3-62-12	132.4	0.282566	0.000019	0.029903	0.000070	0.001119	0.000010	− 7.27	− 4.45	972	1470	− 0.97
SD3-62-13	132.2	0.282486	0.000016	0.026309	0.000293	0.001030	0.000013	− 10.13	− 7.32	1083	1651	− 0.97
SD3-62-14	132.3	0.282496	0.000015	0.021373	0.000320	0.000844	0.000003	− 9.76	− 6.93	1064	1628	− 0.97
91500-6	1064	0.282329	0.000008	0.007341	0.000005	0.000283	0.000000	− 15.67	7.72	1277	1411	− 0.99
GJ-1-6	603	0.282012	0.000008	0.006138	0.000003	0.000247	0.000000	− 26.88	− 13.69	1709	2406	− 0.99

91500, GJ-1, and 610 represent the standard samples

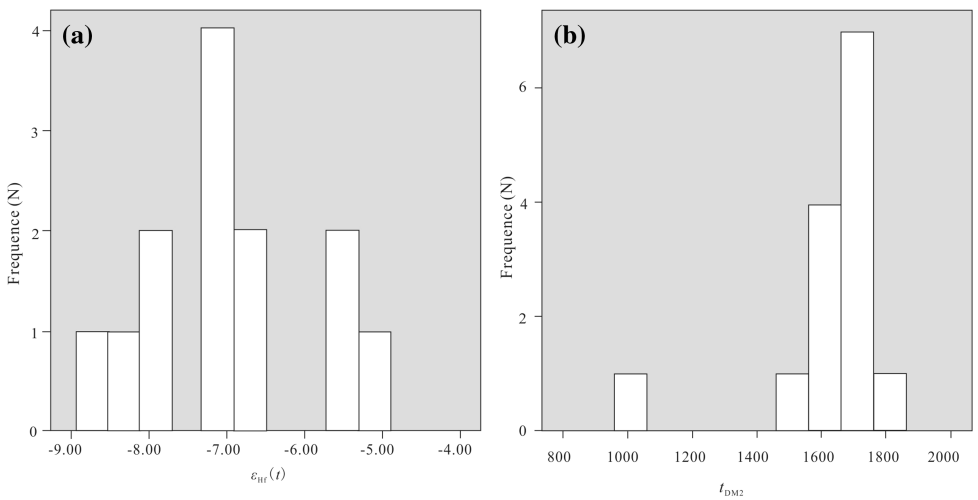

Fig. 8 Histogram of $\varepsilon_{Hf}(t)$ (**a**) and two-stage Hf model age (**b**) of felsite porphyry

5.2 Tectonic setting

In recent years, the tectonic environment and geotectonic setting of magmatic activity in South China became one hotly debated topic and mainly two points of view can be summarized. Some researchers suggested that the magmatic rocks are products of arc-magmatism or syn-orogenic compression environment related to the subduction of the Pacific Plate (Yin et al. 1999; Wang and Deng 2003, 2004). The other group of geologists believed that the magmatic rocks were related to the extension-thinning of the intra-continental lithosphere (Li et al. 1999; Wang et al. 2000). Despite the controversy over "associated with the subduction of the Pacific Plate to the west" and "plate within the lithosphere stretching and thinning effect" on the magma-dynamics tectonic setting of South China in Yanshanian, a growing number of scholars believe that the extension of the lithosphere in South China was initiated in

the Early Yanshanian (Jurassic J_2-J_3) age (Chen et al. 2002, 2004; Wang et al. 2000, 2004; Zhou et al. 2006; Jiang et al. 2009; Zhong et al. 2017a, b). The previous study shows that the magmatic activity in South China in the Cretaceous (Late Yanshanian: K_1) was generated in an extensional environment (Yang et al. 2010; Wang et al. 2019), and characterized by active continental margin arc magma. Jiang et al. (2005) believed that the Xiangshan volcanic-intrusive complex represented alkali-rich, high-temperature A-type magma, which was formed in the back-arc extensional environment related to the subduction of the Paleo-Pacific Plate.

Porphyroclastic rhyolite age (131 ~ 132 Ma) (unpublished), rhyodacite age (135 ~ 136 Ma) (Yang et al. 2010), and the felsite Porphyry age (132 Ma) confirmed that the Xiangshan volcanic-intrusive complex was formed in back-arc extensional stage related to the subduction of Paleo-Pacific Plate toward Asia continent in Cretaceous (Li et al. 2017), when a series of Early Cretaceous fault basins were formed, accompanied by intense emplacement of intermediate-acid magmatic rocks (both intrusive and volcanic), Including the Xiangshan volcanic-intrusive complex.

5.3 Material source of felsite porphyry

Recent researches show that the Xiangshan volcanic-intrusive complex was mainly derived from the partial melting of the crust, with the input of the mantle materials at varying degrees (Fan et al. 2001b; Jiang et al. 2005; Guo et al. 2016). As mentioned above, felsite porphyry shows similar geochemistry characteristics with Xiangshan volcanic rocks and sub-volcanic rocks, suggesting that the felsite porphyry has a nearly consistent magmatic source with Xiangshan volcanic rocks and sub-volcanic rocks. In addition, Yang et al. (2010) reported high initial $^{87}Sr/^{86}Sr$ ratios (0.708837 ~ 0.715208) and lower ε_{Nd} (t) values (− 7.44 to − 8.16) of the rhyodacite, suggesting that the Xiangshan volcanic-intrusive complex is mainly derived from partial melting of the crust material.

Zircon is characterized by strong stability and higher systematical closure temperature of both the U–Pb and Lu–Hf isotopic systems, so the zircons can be used to trace the magmatic sources and illustrating the crust-mantle interaction processes (Griffin et al. 2000, 2002; Soderlund et al. 2004). As mentioned above, the two-stage Hf isotope model ages of felsite porphyry range from 1513 to 1747 Ma (with an average of 1641 Ma), and the ε_{Hf} (t) values range from − 8.82 to − 5.11 (mostly concentrated between − 8 and − 6.5, with one exception of 14.46, Table 2 and Fig. 8a). On ε_{Hf} (t)-$^{206}Pb/^{238}U$ age diagram (Fig. 9), the samples all fell below the chondrite line, indicating that felsite porphyry mainly derived from

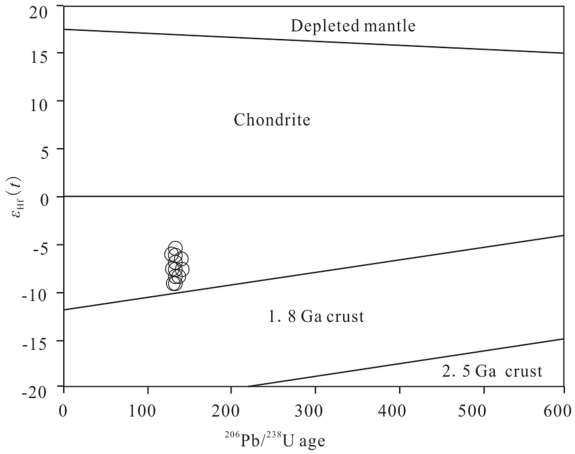

Fig. 9 Zircon $^{206}Pb/^{238}U$ age and $\varepsilon_{Hf}(t)$ diagram of felsite porphyry

partial melting of the metamorphic rocks from the middle Proterozoic basement in the Xiangshan area. In addition, the similar Hf isotope compositions between felsite porphyry and porphyroclastic rhyolite of the Ehuling Formation in mid-western Xiangshan further indicates that the felsite porphyry shares a similar magmatic source with the volcanic-intrusive complex.

Besides the contribution of the crust, the input of the mantle materials has also been discussed in this contribution as follows.

According to Guo et al. (2015, 2016), the two-stage Nd model age (t_{DM2}) of porphyroclastic rhyolite and rhyodacite is about 1.66 Ga and 1.67 Ga, and the $^{207}Pb/^{206}Pb$, $^{207}Pb/^{235}U$, and $^{206}Pb/^{238}U$ model ages of the oldest remaining zircons in the Xiangshan volcanic-intrusive complex are 1655.9 Ma, 1727.7 Ma, and 1787.9 Ma, respectively, which is close to the formation age (1766 ± 19 Ma) of the amphibolite basement rocks of the Cathaysia Block (Li et al. 1998). This indicates that the material sources of the Xiangshan volcanic-intrusive complex dominated by Mesoproterozoic basement metamorphic rocks, also some new mantle-derived material components involved, which result in the general decrease of the Nd model age (Guo et al. 2016).

Apatite is one of the main accessory minerals in granite, and the content of P_2O_5 can distinguish rock type (Bea et al. 1992). P_2O_5 content of I-type and A-type granites decreases with the increase of SiO_2 content, while P_2O_5 content of S-type granites increases or remain unchanged with the increase of SiO_2 (Li et al. 2007). In Fig. 10, there is a negative correlation between P_2O_5 and SiO_2 in the Xiangshan volcanic-intrusive complex, indicating that the magma source is not a single partial remelting event of the metamorphic rocks, some mantle source materials might also involve. In addition, Fan et al. (2005) found mafic microgranular inclusions in the granitic porphyry, which

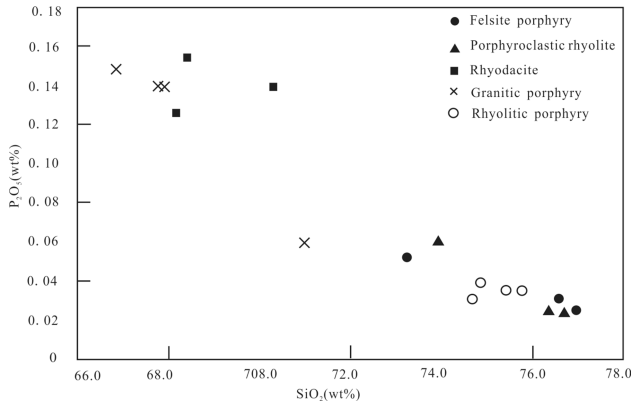

Fig. 10 SiO_2–P_2O_5 scatter diagram of Xiangshan volcanic- intrusive complex

also contained a large number of acicular apatite. The research performed by Yang (2013) shows that the granitic porphyry containing mafic microgranular inclusions and porphyroclastic rhyolite, rhyodacite without mafic microgranular inclusions, have similar Nd-Hf isotopic compositions, which is further regarded to be the basic and acidic magma mixing process due to the large temperature differences between two kinds of magmas, although the magmatic mixing might only occur in shallow parts, with relatively less contribution of the mantle materials.

All the above evidence indicates that the formation of the Xiangshan volcanic-intrusive complex is not only related to the partial melting of the crust, but also the input of small amounts of mantle materials. It is concluded that the felsite porphyry is mainly related to the partial melting of Mesoproterozoic basement metamorphic rocks, with the input of small amounts of the mantle materials.

6 Conclusions

1. LA-ICP-MS zircon U–Pb dating of felsite porphyry yielded a mean $^{206}Pb/^{238}U$ age of 132.2 ± 0.9 Ma, which is close to that of the porphyroclastic rhyolite.
2. Felsite porphyry shares similar geochemistry characteristics and zircon Hf isotopic compositions with other volcanic rocks of the Xiangshan volcanic-intrusive complex (especially porphyroclastic rhyolite), suggesting that they are the products of the same magmatic activity in different stages.
3. Xiangshan volcanic-intrusive complex, including the felsite porphyry, was formed at the back-arc extension settings related to the subduction of the Pacific late toward the Asia continent, and they are mainly formed by partial melting of the Mesoproterozoic basement metamorphic rocks, with the input of the small amount of mantle materials.

Acknowledgements This study is supported by "Comprehensive Study of 3D Metallogenic Geologic Environment of Key Zones for Exploration in Xiangshan Uranium Orefield", the sub-project of "Longcan Science and Technology Innovation Demonstration Project" of China National Nuclear Corporation (Project No.: LCD116).

References

Anderson T (2002) Correction of common lead in U–Pb analyses that do not report ^{204}Pb. Chem Geol 192(1–2):59–79

Bea F, Fershtater G, Corretge LG (1992) the geochemistry of phosphorus in granite rocks and the effect of aluminium. Lithos 29(1/2):43–56

Blichert TJ, Albarede F (1997) The Lu–Hf isotope geochemistry and planetary of chondrites and the evolution of the mantle-crust system. Earth Sci Lett 148(1–2):243–258

Chen XM, Lu JJ, Liu CS et al (1999) Single-grain zircon U–Pb isotopic ages of the volcanic-intrusive complexes in Tonglu and Xiangshan areas. Acta Petrol Sin 15(2):272–278 (**in Chinese with English Abstract**)

Chen PR, Hua RM, Zhang BT et al (2002) Post-orogenic granitoids of early Yanshanian of Nanling: petrological constraints and geochemical dynamics background. Sci China (Ser D) 32(4):279–289 (**in Chinese**)

Chen PR, Zhou XM, Zhang WL et al (2004) Genesis and significance of Early Yanshanian syenite-granite complex in the Eastern Nanling. Sci China (Ser D) 34(6):493–503 (**in Chinese**)

Chen ZL, Wang Y, Zhou YG et al (2013) SHRIMP U–Pb dating of zircons from volcanic-intrusive complexes in the Xiangshan Uranium Orefield, Jiangxi Province, and its geological implications. Geology in China 40(1):217–228 (**in Chinese with English Abstract**)

Fan HH, Ling HF, Shen WZ et al (2001a) Nd-Sr-Pb isotope geochemistry of the volcanic-intrusive complex at Xiangshan, Jiangxi Province. Acta Petrol Sin 17(3):395–402 (**in Chinese with English Abstract**)

Fan HH, Wang DZ, Liu CS et al (2001b) Discovery of quenched enclaves in Subvolcanic rocks in Xiangshan, Jiangxi Province and its genetic mechanism. Acta Geol Sin 75(1):64–69 (**in Chinese with English Abstract**)

Fan HH, Wang DZ, Shen WZ et al (2005) Formation age of the intermediate-basic dikes and volcanic-intrusive complex in Xiangshan, Jiangxi Province. Geol Rev 51(1):86–91 (**in Chinese with English Abstract**)

Fan HH, Wang X, Wang DZ et al (2009) Study on mineralogical characteristics of volcanic-intrusive complex in Xiangshan, Jiangxi Province and its tracer significance. Acta Mineral Sin S1:8–9 (**in Chinese**)

Fang XH, Hou WY, Wan GL (1982) Petrographic studies of the volcanic complex in the Xiangshan Caldera. Mineral et Anal 1(1):1–10 (**in Chinese with English Abstract**)

Fernando C, John MH, Paul WOH et al (2003) Atlas of zircon textures. Rev Mineral Geochem 53(12):469–500

Griffin WL, Pearson NJ, Belousova E et al (2000) The Hf isotope composition of Cratonic mantle: LA-MC-ICP-MS analysis of zircon megacrysts in kimberlites. Geochim Cosmochim Acta 64(1):133–147

Griffin WL, Wang X, Jackson SE et al (2002) Zircon chemistry and Magma mixing, SE China: in-situ analysis of Hf isotopes, Tonglu, and Pingtan igneous complexes. Lithos 61(3–4):237–269

Guo J, Li ZY, Huang ZZ et al (2014) Determination of felsite porphyry in Xiangshan uranium ore field and its geological significance. Mineral Deposits S1:195–196 (**in Chinese**)

Guo FS, Yang QK, Xie CF et al (2015) Zircon geochronology and evolution sequence of the acidic volcano-intrusive complex from Xiangshan, Jiangxi Province. Chin J Geol 50(3):684–707

Guo FS, Yang QK, Meng XJ et al (2016) Geochemical characteristics and petrogenesis of the acidic volcanic-intrusive complexes, Xiangshan, Jiangxi. Acta Geol Sin 90(4):769–784 (**in Chinese with English Abstract**)

He GS, Dai MZ, Li JF et al (2009) SHRIMP Zircon U-Pb dating and its geological implication for the Xiangshan porphyric dacite-rhyolitic. Geotecton Metallog 33(2):300–305 (**in Chinese with English Abstract**)

Hou KJ, Li YH, Zou TR et al (2007) Laser ablation-MC-ICP-MS technique for Hf isotope microanalysis of zircon and its geological applications. Acta Petrol Sin 23(10):2592–2604 (**in Chinese with English Abstract**)

Jiang YH, Ling HF, Fan HH et al (2005) Petrogenesis of a late jurassic peraluminous volcanic complex and its high-Mg, potassic, quenched enclaves at Xiangshan, Southeast China. Petrol 46(6):1121–1154

Jiang YH, Jiang SY, Dai BZ et al (2009) Middle to late jurassic felsic and mafic magmatism in southern Hunan Province, Southeast China: implications for a continental orc to rifting. Lithos 107(3–4):185–204

Le Maitre RW, Bateman P, Dudek A et al (1989) Igneous rocks: IUGS classification and glossary recommendations of the international union of geological sciences, subcommission on the systematics of igneous rocks. Blackwell Scientific Publications, London, pp 23–58

Li XH, Wang YX, Zhao ZH et al (1998) SHRIMP U-Pb zircon geochronology for amphibolite from the precambrian basement in SW Zhejiang and NW Fujian Province. Geochimica 27(4):327–334 (**in Chinese with English Abstract**)

Li XH, Zhou HH, Liu Y et al (1999) Petrology and geochemistry characteristics of the potassium metaphysic intrusive zone in southeast Guangxi. Sci Bull 44(18):1992–1998 (**in Chinese**)

Li XH, Li WX, Li ZX (2007) On the genetic classification and tectonic implications of the early Yanshanian granitoids in the Nanling range, South China. Chin Sci Bull 52(14):1873–1885

Li ZY, Huang ZZ, Li XZ et al (2014) Xiangshan igneous rock and uranium mineralization. Beijing: Geological publishing house, pp15–58 (in Chinese)

Li SZ, Zeng YB, Wang PC, et al (2017) Mesozoic tectonic transition in South China and initiation of palaeo-pacific subduction. Earth Sci Front 24(4):213–225 (**in Chinese with English Abstract**)

Liu CS, Zhu JC, Shen WZ et al (1990) Classification and source materials of continental crust transformation series granitoids in South China. Acta Geol Sin 64(1):43–52 (**in Chinese with English Abstract**)

Ludwing KR (2003) ISOPLOT 3.0: a geochronology toolkit for microsoft excel. Berkeley: Berkeley Geochronology Center. Special Publication, pp 1–53

Ruan XY (2018) Petrography, geochemistry, geochronology and the research significance of Wuzhang Granitic Porphyry in Southern Xiangshan, Jiangxi Province. [Master degree thesis], Jiangxi: East China University of technology, pp1–35 (**in Chinese**)

Samuel AB, Mark DS (2003) High-precision U–Pb zircon geochronology and the stratigraphic record. Rev Mineral Geochem 53(12):305–326

Si ZF, Li ZY, Nie JT et al (2018) Characteristics of the rhyolite porphyry at Heyuanbei in Xiangshan uranium orefield, Jiangxi province. Geoscience 32(1):45–55 (**in Chinese with English Abstract**)

Soderlund U, Patchett PJ, Vervoort JD et al (2004) The ^{176}Lu decay constant determined by Lu–Hf and U–Pb isotope systematics of precambrian mafic intrusions. Earth Planet Sci Lett 219(3–4):311–324

Song B, Zhang YH, Liu DY (2002) Introduction to the naissance of SHRIMP and its contribution to isotope geology. J Chin Mass Spectrom Soc 23(1):58–62 (**in Chinese with English Abstract**)

Sun SS, McDonough WF (1989) Chemical and isotopic systematics of oceanic basalts: implications for mantle composition and processes. Geol Soc Lond Spec Publ 42(1):313–345

Wang YJ (2015) Characteristics of Xiangshan Granitic Porphyry and Basic-intermediate Dikes and their Relationship with Uranium Mineralization. [Master degree thesis]. Beijing: Beijing Research Institute of Uranium Geology, pp10–58(**in Chinese with English Abstract**)

Wang Y, Deng JF (2003) Geodynamic implication of petrochemical features of Yanshanian strongly peraluminous granitoids in Wuchang-Sihui fracture belt of Guangdong. Geotectonica et Mitallogenia 27(1):56–63 (**in Chinese with English Abstract**)

Wang Y, Deng JF (2004) Petrochemical features and tectonic setting of late Yanshanian strongly peraluminous granites in the northeastern part of Hunan Province. Geotectonica et Mitallogenia 28(1):60–68 (**in Chinese with English Abstract**)

Wang DZ, Liu CS, Shen WZ et al (1991) Discovery and geological significance of mesozoic S-type volcanic belt in Xiangshan, Dongxiang-Xiangshan Area, Jiangxi Province. Sci Bull 36(19):1491–1493 (**in Chinese**)

Wang YJ, Fan WM, Guo F et al (2000) Petrological and geochemical characteristics of mesozoic granodioritic intrusions in southeast Hunan Province. China Acta Petrol Sin 17(1):169–175 (**in Chinese with English Abstract**)

Wang YJ, Liao CL, Fan WM et al (2004) Early mesozoic OIB-type alkaline basalt in Central Jiangxi province and its tectonic implications. Geochimica 33(2):109–117 (**in Chinese with English Abstract**)

Wang YJ, Lin JR, Hu ZH et al (2019) Zircon U–Pb Geochronology, Geochemistry and Hf Isotopic Compositions of Dacitic Porphyry in Zoujiashan Deposit of Xiangshan Uranium Orefield and its Geological Implication. Earth Science, [2020–1–21] http://kns.cnki.net/kcms/detail/42.1874.P.20191104.0935.006.html

Wright JB (1969) A simple alkalinity ratio and its application to questions of nonorogenic granite genesis. Geol Mag 106(4):370–384

Wu RG (1999) The features of volcanic formation in Ruyiting profile of Xiangshan. J East China Geol Inst 22(3):201–208 (**in Chinese with English Abstract**)

Wu RG, Yu DG, Zhang SM (2003) Identification of rhyolite-dacite porphyry and its relation to uranium mineralization at Xiangshan uranium orefield. Uranium Geol 19(2):81–87 (**in Chinese with English Abstract**)

Wu FY, Li XH, Zheng YF et al (2007) Lu–Hf isotopic systematics and their applications in petrology. Acta Petrol Sin 23(2):185–220 (**in Chinese with English Abstract**)

Wu JH, Lao YJ, Xie GF et al (2017) Stratigraphy and geochronology of the volcanic rocks in the Xiangshan uranium orefield, Jiangxi Province, and its geological implications. Geol China 44(5):974–992 (**in Chinese with English Abstract**)

Xia LQ, Xia ZC, Zhang C, et al (1992) Rock geochemistry of mesozoic uranium-bearing volcanic complex, Xiangshan. Beijing: Geological publishing house, pp 1–97 (**in Chinese**)

Yang SY (2013) Petrogenesis and Geodynamic Setting of Magmatic Rocks from Uranium-bearing Volcanic Basins, Gan-Hang Belt, Southeast China. [Doctor degree thesis], Nanjing: Nanjing University, pp 15–58 (in Chinese with English Abstract)

Yang SY, Jiang SY, Jiang YH et al (2009) Zircon U–Pb precision dating of volcanic complex intrusions in Xiangshan, Jiangxi

province and its geological significance. Acta Mineralogica Sin S1:341–342 (**in Chinese**)

Yang SY, Jiang SY, Jiang YH et al (2010) Zircon U–Pb geochronology, Hf isotopic composition and geological implications of the rhyodacite and rhyodacitic porphyry in Xiangshan Uranium Orefield, Jiangxi Province, China. Sci Chin Earth Sci 40(8):953–969 (**in Chinese**)

Yang SY, Jiang SY, Jiang YH et al (2011) Geochemical, constraints on zircon U–Pb dating and Sr–Nd–Hf isotopic the age and petrogenesis of an early cretaceous volcanic-intrusive complex at Xiangshan, Southeast China. Miner Petrol 101(1–2):21–48

Yin HF, Wu SB, Du YS et al (1999) South China defined as part of tethyan archipel agic ocean system. Earth Sci 24(1):1–12 (**in Chinese with English Abstract**)

Yu DG (2001) Prospecting ideas for mesozoic granite-type, volcanic-type and exocontact-type uranium deposits in South China(I). Uranium Geol 17(5):257–265 (**in Chinese with English Abstract**)

Yu ZQ, Chen WF, Chen PR et al (2019) Chemical composition and Sr isotopes of apatite in the Xiangshan A-type volcanic-intrusive complex, Southeast China: new insight into petrogenesis. J Asian Earth Sci 172:66–82

Zhang WL (2011) Exploration on the preservation factors of uranium deposits in South China. Beijing: Geological publishing house, pp1–190 (**in Chinese**)

Zhang WL (2016) New understanding of the genesis of cryptoexplosive intrusive rocks-Xiangshan. Jiangxi Geol 17(3):184–189 (**in Chinese with English Abstract**)

Zhang WL, Li ZY (2007) Single-zircon U–Pb age of rhyodacite from Xiangshan area and its geological implications. Acta Petrol et Mineralogica 26(1):21–26 (**in Chinese with English Abstract**)

Zhang WL, Gao MQ, Lyu C et al (2018) Zircon LA-ICP-MS U-Pb dating and its geological significance in Lujing Area of Hunan and Jiangxi border. Geol Surv Res 41(3):161–166 (**in Chinese with English Abstract**)

Zhong J, Pirajno F, Chen YJ (2017a) Epithermal deposits in South China: geology, geochemistry, geochronology, and tectonic setting. Gondwana Res 42:193–219

Zhong J, Chen YJ, Pirajno F (2017b) Geology, geochemistry and tectonic settings of the molybdenum deposits in South China: a review. Ore Geol Rev 81:829–855

Zhou XH, Wang ZN (2012) Characteristics and genesis of porphyroclastic Lava Rock in Xiangshan. Uranium Geol 28(2):72–79 (**in Chinses with English Abstract**)

Zhou XM, Sun T, Shen WZ et al (2006) Petrogenesis of mesozoic granitoids and volcanic rocks in South China: a response to tectonic evolution. Episodes 29(1):26–33

Mingming Tian male, born in 1987 in Weinan city, Shanxi Province, China; master, graduated from Beijing Research Institute of Uranium Geology, engineer. He is now interested in exploration and evaluation of volcanic type of uranium/thorium resources.